Journal of Physics: Conference Series

PAPER • OPEN ACCESS

Temperature decrease and multiple acceleration of structural and phase transformations in metastable metals and alloys under cascade-forming irradiation. Part 2 – Experimental Results and Discussion

IOP Conf. Series: Journal of Physics: Conf. Series **1115** (2018) 032047 doi:10.1088/1742-6596/1115/3/032047

Temperature decrease and multiple acceleration of structural and phase transformations in metastable metals and alloys under cascade-forming irradiation. Part 2 – Experimental Results and Discussion

V V Ovchinnikov[1,2]

[1]Institute of Electrophysics, Ural Branch, Russian Academy of Sciences, 106 Amundsen Str., Ekaterinburg, 620016, Russia
[2]Ural Federal Technical University named after the First President of Russia B.E. Yeltsin, 19 Mira Str., Yekaterinburg, 620002, Russia

E-mail: viae05@rambler.ru

Abstract. Part 2 is a continuation of Part 1 of the Review and presenting examples of recent research by the author and his colleagues which confirm the main features of low-dose processes caused by nanoscale dynamic effects under cascade-forming irradiation, namely:(1) a decrease in the temperature of structural and phase transformations by 100-300 K in pure metals and alloys which were initially in nonequilibrium (amorphous, strongly deformed, quenched) states; (2) repeatedly (by 2-3 or more orders of magnitude) increase in the flow rate as compared with thermoactivated processes; (3) propagation of transformations over distances many times exceeding the projected ranges (R_p) of ions (or the ranges of primary recoil atoms under neutron irradiation); theoretically, these distances are unlimited, in practice they reach $(10^3\text{-}10^5)\cdot R_p$ and more (up to several mm in aluminum alloys). In the near future, the observed effects may provide a breakthrough in fundamental studies of low-temperature processes in metastable media as well as in processing and design of new functional materials.

1. Introduction
In Part 2 of the Review, the latest experimental data which testify to the significant role of nanoscale dynamic effects under cascade-forming irradiation of metastable media by heavy accelerated ions are considered. The results of direct observation of thermal spikes regions heated to temperatures exceeding the melting point of metals are presented.

2. On the experimental procedure
Irradiation by continuous beams of N^+, Ar^+ and Xe^+ ions was carried out using an ILM-1 ion implanter equipped with two ion sources PULSAR-1M based on a low-pressure glow discharge [1] (which can operate in a continuous an/or pulse-repetitive millisecond mode) at the Institute of Electrophysics of the UB RAS (Ekaterinburg, Russia).

During all experiments, the temperature of the targets was monitored in order to separate the thermal and radiation effects.

IOP Conf. Series: Journal of Physics: Conf. Series **1115** (2018) 032047 doi:10.1088/1742-6596/1115/3/032047

3. Experimental results and discussion

3.1. Nanoscale dynamic effects under cascade-forming irradiation, instantaneous rearrangement of condensed matter at low temperatures; long-range effects

Shown in figure 1 are the types of metastable metallic materials, the results of research of which are the subject of this Review. In this figure, the regularities found already in the first experiments on the effect of ion beams on nonequilibrium media [2-7] and confirmed in subsequent studies are noted. The radiation-induced transformations predicted by the theory and experimentally observed in metastable media are shown in figure 2 (1-5). They proceed at a high rate at low temperatures and at anomalously large distances from the irradiated surface (up to 10^4-10^5 projected ion ranges and more), which can not be explained within the framework of traditional concepts. Such transformations include: (1) non-diffusion martensitic transformations in systems with limited diffusion at a lower temperature [3-5, 8]; (2) formation of short-range and long-range atomic order (in metastable alloys disordered by quenching or cold plastic deformation) [2, 4-6, 8, 9-12]; (3) crystallization of amorphous alloys [13]; (4) decay of supersaturated solid solutions (and reverse processes of accelerated phase dissolution) [14-18]; and (5) polygonization and recrystallization of cold-rolled alloys [16–20].

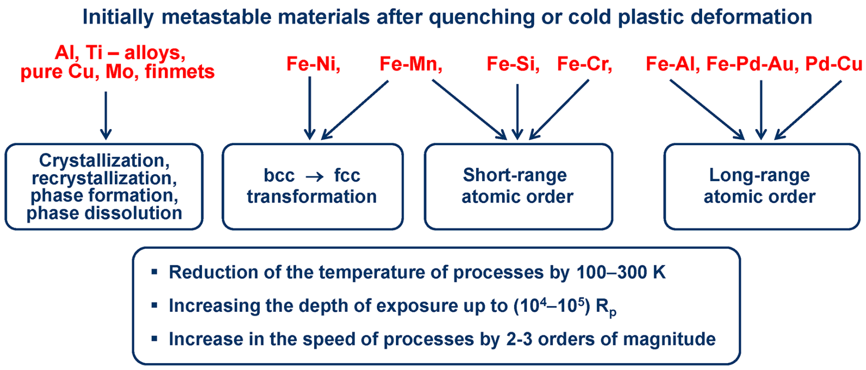

Figure 1. Objects of research. The main advantages of ion-beam processing of these materials with the use of radiation-dynamic effects.

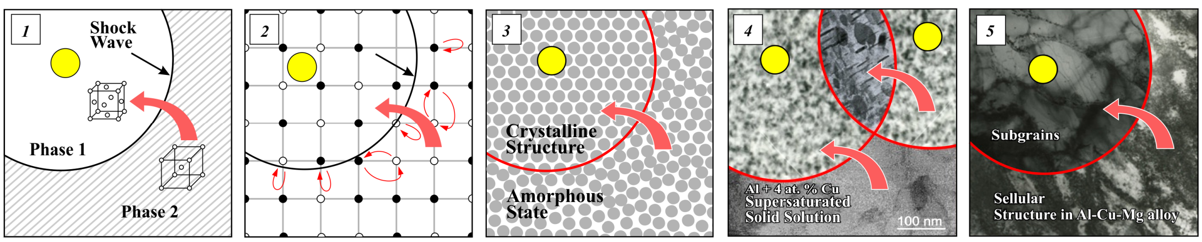

Figure 2. Structural-phase transformations in metastable media under ion irradiation.

Part 1 of the review outlines the ideas pertaining to nanoscale dynamic effects in cascade-forming irradiation of nonequilibrium media. Given below are the latest experimental data proving the essential, and in some cases decisive, role of these effects in the formation of the structure and phase composition of metal targets under ion irradiation.

3.2. Influence of ion irradiation on the nanocrystallization of a soft magnetic amorphous alloy $Fe_{72.5}Cu_1Nb_2Mo_{1.5}Si_{14}B_9$

The influence of ion bombardment (Ar +; *E*=30 keV, *j*=300 μA/cm2) on the process of volume crystallization and the magnetic properties of amorphous ribbons of $Fe_{72.5}Cu_1Nb_2Mo_{1.5}Si_{14}B_9$ alloy was studied in [13]. Ribbons with a thickness of 25 μm were obtained by super-high melt quenching . The studies were carried out with the help of X-ray diffraction analysis, transmission electron microscopy, and also using thermomagnetic and other magnetic methods.

It was shown that irradiation for only 2 s (fluence $3.75\cdot10^{15}$ cm^{-2}) causes a short-term heating of the ribbons to 620 K, which is 150 K below the threshold of thermal crystallization of this alloy (~ 770 K). Nevertheless, ion bombardment leads to complete nanocrystallization of the entire volume of the ribbons with formation of a solid solution of α-Fe (Si) ($Fe_{80}Si_{20}$), a stable phase of Fe_3Si, and hexagonal phases

Amorphous ribbons during their irradiation were moved under a beam of argon ions with a cross section of 20×100 mm^2 at a speed of 1 cm/s. This means that each point of these ribbons was was exposed to a beam exactly during 2 seconds.

Figures 3a-d show X-ray patterns obtained from magnetic ribbons $Fe_{72.5}Cu_1Nb_2Mo_{1.5}Si_{14}B_9$ alloy, 25 μm thick and 10 mm wide. The X-ray diffractogram of the initial ribbons obtained by melt quenching (figure 3a) shows only the amorphous halo. Analysis of the X-ray diffraction pattern of the sample annealed in the furnace at 840 K during 1 h revealed two phases only, one of which is α-Fe and the other is the superstructure of Fe_3Si (figure 3b).

It can be seen that the state formed with such short-term irradiation at a lower temperature is closer to equilibrium compared to the state after standard annealing in the furnace. Narrow lines are observed and more phases are formed. X-ray diffraction patterns are the same for both sides of the ribbons. The obtained state is highly stable and does not change during the subsequent standard annealing in the furnace (840 K, 1 h) (figure 3d).

Scanning electron and atomic force microscopy confirm that nanocrystallization takes place in the entire volume of irradiated ribbons [13, 21]. Preliminary studies showed a high sensitivity of the magnetic properties of the investigated ribbons to the regime of ion irradiation (radiation annealing), which can be used to obtain the desired magnetic properties (hysteresis loop shapes, saturation induction, and magnetization reversal losses at different frequencies).

Previously, a significant effect of radiation treatment on the atomic and magnetic structures of transformer steels, permalloy and nanocrystalline soft magnetic materials (finemets) [8, 22-24] was discovered. In particular, the optimization of the Ar^+ irradiation regimes of $Fe_{72.5}Cu_1Nb_3Mo_{1.5}Si_{13.5}B_9$ alloy (previously subjected to standard annealing) [22-24] allowed, due to the creation of a more balanced structure, to reduce magnetization reversal losses by 10% at frequencies from 50 to 10 000 Hz.

3.3. The fast-flowing volume decomposition of the supersaturated solid solution Al-4 wt % Cu under irradiation with accelerated Ar^+ ions

A supersaturated solid solution of the Al-4 wt % Cu alloy quenched from 520°C is a classic example of a metastable medium. At temperatures T >150-200°C, this alloy decomposes with the precipitation of copper-rich θ' and θ phases. An investigation of the effect of ion bombardment on this alloy was carried out in [14, 15].

The authors of these studies found the multiple-accelerated decay of a supersaturated solid solution of Al-4 wt % Cu (formed as a result of quenching from 520°C), with the precipitation of θ'', θ' and θ phases under irradiation with Ar^+ ions (E=20 keV, j=160 μA/cm^2). The temperature of the samples during irradiation did not exceed 60°C. Analogous changes during thermal annealing are observed only at temperatures exceeding 150-200°C.

A significant increase in the microhardness of a layer of depth no less then 6-8 μm is observed even as a result of irradiation with a duration of only 1 s ($F=1\cdot10^{15}$ cm^{-2}, T<25 °C).

The change in the lattice parameter (according to X-ray diffraction data) indicates a change in the structural state of the layer with a thickness of at least 50 µm. The HREM method demonstrates the formation of the Guinier-Preston zones and the precipitation of the phases θ' and θ (figure 4), at such low temperature and during only a few seconds of irradiation, while prolonged aging in the absence of irradiation (60 °C, 8 h) causes in these conditions only a zonal stage of decay with the formation of the Guinier-Preston zones.

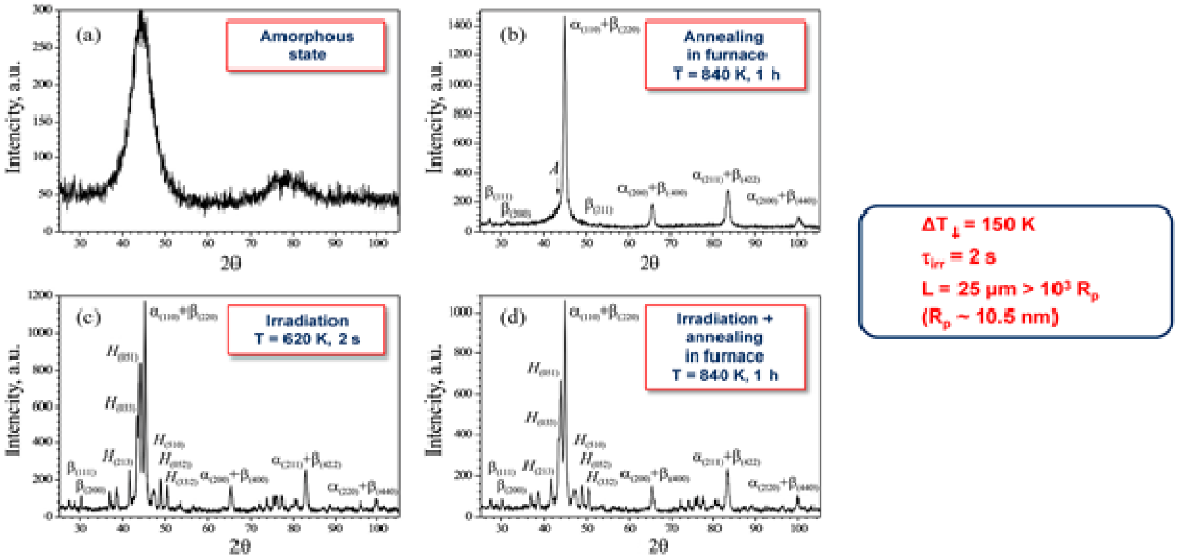

Figure 3. Instantaneous nanocrystallization of alloy $Fe_{72.5}Cu_1Nb_2Mo_{1.5}Si_{14}B_9$ under Ar^+ irradiation (E = 30 keV, j = 300 µA/cm^2, F=3.7·10^{15} cm^{-2}): (a) amorphous state; (b) annealing in furnace T=840 K, 1 h; (c) irradiation T=620 K, 2 s; (d) irradiation plus annealing T=840 K, 1 h [13, 21].

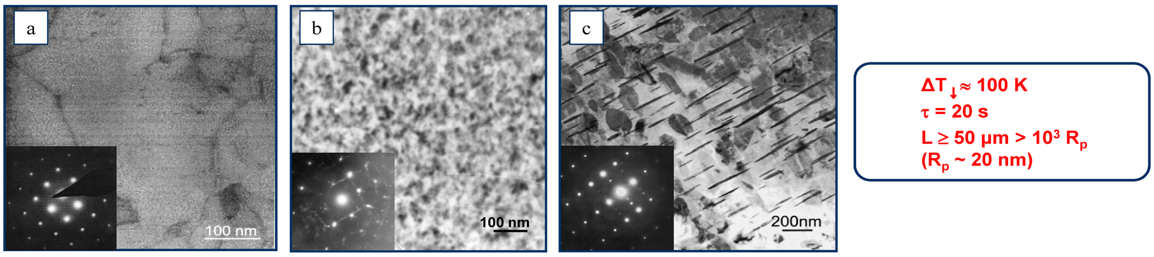

Figure 4. Microstructure of the Al-4 wt % Cu: (a) initial state: quenching from 520°C; (b) aging: T=60 °C, t=8 h; (c) irradiation with Ar^+ ions: 20 keV, 160 µA/cm^2, F=2·10^{16} cm^{-2} (T<25°C, t=20 s) [15].

3.4. Examples of modification of the properties of industrial aluminum alloys

The effect of ion bombardment on the structure, phase composition, and mechanical properties of strips of industrial aluminum alloys AMg$_6$ (Al-Mg), 1441 (Al-Li-Cu-Mg), 1424 (Al-Li -Mg-Zn), 1960 (Al-Zn-Mg-Cu), VD1 (Al-Cu-Mg) with Mn additives depending on the ion energy, ion current density, dose and irradiation temperature was studied. The thermal effect of the ion beam was simulated by heating the samples in a muffle furnace, oil or salt baths. It is shown that at T << T_{ann} (T_{ann} is the standard annealing temperature in a furnace), no changes in the structure and properties of the alloys occur in the absence of irradiation. In the same conditions, the beams of accelerated Ar+ ions initiate repeatedly accelerated radiation annealing (in comparison with furnace annealing) in cold-rolled (ε=40-70 %) alloys AMg$_6$, 1441, 1424 and VD1. Radiation annealing occurs at lower temperatures (in some cases at 150-200 K below the temperature of standard annealing) in the entire volume of strips 1-7.5 mm thick (the average projected range of 20-40 keV Ar^+ ions in aluminum alloys is ~20-40 nm).

It is shown that radiation annealing by powerful continuous Ar+ ion beams leads to the following processes:

– polygonization with the formation of subgrains (at fluences of 10^{15}-10^{16} cm^{-2} (corresponding irradiation time ≤1-4 s at j=400 $\mu A/cm^2$);

– dissolution (10^{15} cm^{-2}) and formation (10^{16}-10^{17} cm^{-2}) of new phases;

– recrystallization and growth of grains ($5 \cdot 10^{16}$-10^{17} cm^{-2} or more) and like annealing in a furnace, ion bombardment eliminates the crystallographic texture [20].

The dependences of the tensile strength σ_u, yield stress $\sigma_{0.2}$, and the relative elongation δ of the AMg_6, 1441 and VD1 alloys on the ion energy, ion current density, and irradiation dose were studied in detail. Using the regression analysis, the analytical multidimensional dependences σ_u (E, j, D), $\sigma_{0.2}$ (E, j, D) and δ (E, j, D) as a functions of the ion beam parameters were obtained.

3.5. Observation of zones of thermal spikes on the surface of Ni and $Fe_{0.56}Ni_{0.44}$ nanowires

The radiation resistance of nanowires (NWs) 60 and 100 nm in diameter from pure nickel and $Fe_{0.56}Ni_{0.44}$ iron-nickel alloy under irradiation with continuous beams of Ar^+ and Xe^+ (E=20 keV, j=300 $\mu A/cm^2$) ions was investigated in [25]

During irradiation, NWs were fixed on a copper substrate (figure 5a) with a rotating holder (the angle between the axis of the ion beam and the normal to the surface of the substrate was 45°C). Fluence range: F=10^{16}-10^{18} cm^{-2}. The substrate temperature did not exceed 550°C.

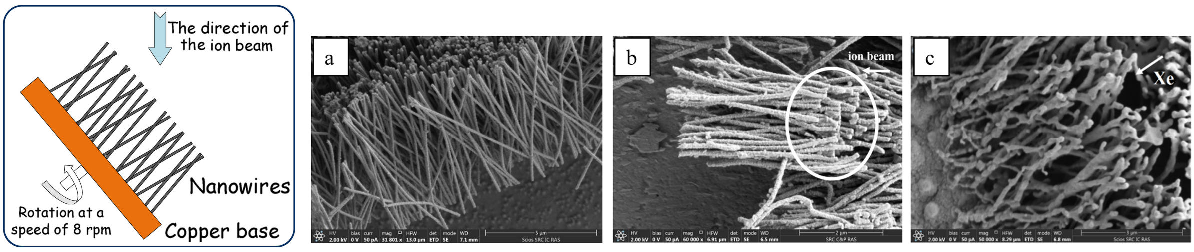

Figure 5. Local melting of nanowires from $Ni_{56}Ni_{44}$ alloy 60 nm thick in the regions of thermal spikes during irradiation with Ar^+ and Xe^+ ions: (a) – initial state, (b) – after Ar^+ irradiation, (c) – after Xe^+ irradiation [25].

The experiments carried out made it possible to prove the presence and important role of thermal spikes the diameter of which (~ 5–10 nm) is comparable to the diameter of the nanowires studied. The Scanning Electron Microscope (SEM) detected local molten zones on the surface of the NWs made both of pure nickel and of the alloy, as well as bending and damage of these NWs (figures 5bc).

As shown in Part 1 of the review, the regions of passage of dense cascades of atomic displacements are thermalized for ~10^{-12} s (cooling time ~10^{-11} s) and can be heated up to 6000 K and higher. The average calculated depth at which these regions form in examined NWs is about 5-10 nm at an ion energy of 20 keV.

SEM images show the formation of molten zones on the surface of the NWs in the form of buds (kidneys) and even branches under ion irradiation (figures 5bc). Local melting of nanowires of pure nickel and iron-nickel alloy $Fe_{0.56}$ $Ni_{0.44}$, (without complete melting of all NWs) proves the formation of thermal spikes under irradiation with heavy ions considered in [5, 15]. In this case, surface chips and splashing of the regions of thermal spikes from nanowires are possible. As a result of the propagation of powerful postcascade waves, the NWs can be broken and bent. Since the energy release per cascade atom for Xe^+ is much larger than for Ar^+ [25], in the case of Xe^+ irradiation, a more significant bending of the nanowires is observed. In this case, the adjacent nanowires can be covered with molten metal.

4. Conclusion

In the world literature there is a significant number of publications using, the term "long-range effects" in connection with the implantation of accelerated ions into the substance. They relate to effects of a very varied origin [26].

The nanoscale dynamic effects considered in the review are of a completely different nature. Being observed at low radiation doses, these processes have very short characteristic times, high local pressures and temperatures capable of initiating self-propagating structural and phase transformations in nonequilibrium media [6, 27].

This determines:

– decrease in the temperature of the processes by 100-300 K,

– increase in the depth of influence up to (at least up to 10^4-10^5) R_p,

– increase in the rate of processes by 2-3 and more orders of magnitude.

In general, there is reason to believe that the research and use of dynamic effects caused by ion bombardment can be a breakthrough in fundamental concepts and the creation of new materials with substantially improved and unique properties in the near future.

Acknowledgments

The work was fulfilled in the frame of state task project № 0389-2015-0025, supported by the Act 211 of the Government of the Russian Federation (Agreement No. 02.A03.21.0006) and it was supported by the Russian Scientific Foundation, project no. 15-19-10054 (sections 3.1 and 3.4)

References

[1] Gavrilov N V, Mesyats G A, Nikulin S P et al 1996 *J. Vac. Sci. Technol.* **A14** 1050
[2] Borodin S N, Kreindel Yu E, Mesyats G A, Ovchinnikov V V 1989 *Pis’ma v zhurn. tekhn. fiz.* **15** 87
[3] Borodin S N, Kreindel Yu E, Mesyats G A, Ovchinnikov V V et al 1989 *Pis’ma v zhurn. tekhn. fiz.* **15** 51
[4] Ovchinnikov V V, Chernoborodov V I, Ignatenko Yu G 1995 *Nucl. Instrum. and Meth. in Phys. Res. B* **103** 313
[5] Ovchinnikov V V, Kogan Yu D, Gavrilov N V, Shtoltz A K 1994 *Surf. and Coat. Technol.* **64** 1
[6] Ovchinnikov V V 1994 *Proceedings XVI International Symposium on Discharges and Electrical Insulation in Vacuum* (Moscow-St. Petersburg. SPIE) **2259** 605
[7] Ovchinnikov V V 1996 *Russ. Metall.* **6** 90
[8] Ovchinnikov V V 2008 *Phys.–Usp.* **51** 955
[9] Goloborodsky B Yu, Ovchinnikov V V and Semenkin V A 2001 *Fusion Technol*. **39** 1217
[10] Ovchinnikov V V, Gushchina N V and Ovchinnikov S V 2015 *Phys. Met. Metallogr.* **116** 1234
[11] Ovchinnikov V V, Goloborodsky B Yu, Gushchina N V, Semionkin V A and Wieser E 2006 *Appl. Phys. A.* **83** 83
[12] Ovchinnikov V V, Chernoborodov V I and Ignatenko Yu G 1995 *Nucl. Instrum. and Meth. in Phys. Res. B* **103** 313
[13] Ovchinnikov V V, Makhin’ko F F, Gushchina N V et al 2017 *Phys. Met. Metallogr.* **118** 150
[14] Mücklich A, Gushchina N, Wieser E and Ovchinnikov V V 2003 *31th Proc. Conference of the DGE. Deutsche Gesellschaft für Elektronenmikroskopie, Dresden* 348
[15] Gushchina N V, Ovchinnikov V V, Mücklich A. 2016 *Phys. Stat. Sol. B* **253** 770
[16] Ovchinnikov V V, Gushchina N V, Makhin’ko F F, Chemerinskaya L S et al 2008 *Phys. Met. Metallogr.* **105** 375
[17] Ovchinnikov V V, Gavrilov N V, Gushchina N V et al 2010 *Russ. metall. (Metally)* **3** 207
[18] Ovchinnikov V V, Remnev G E, Gushchina N V et al 2011 *Russ. J. of Non-Ferr. Met.* **52** 304
[19] Ovchinnikov V V, Gushchina N V, Mozharovsky S M and Kaigorodova L I 2017 *IOP Conf. Ser.: Mater. Sci. and Eng.* **168** 012067
[20] Ovchinnikov V V, Gushchina N V, Titorov D B et al 2010 *Phys. Met. Metallogr.* **109** 77

IOP Conf. Series: Journal of Physics: Conf. Series **1115** (2018) 032047 doi:10.1088/1742-6596/1115/3/032047

[21] Romanov I Yu, Gushchina N V, Ovchinnikov V V et al 2018 *Russian Physics Journal*. **60** 1823
[22] Sokolov B K, Gubernatorov V V, Dragoshanskii Yu N et al 2000 *Phys. Met. Metallogr.* **89** 348
[23] Dragoshanskii Yu N, Gubernatorov V V, Sokolov B K and Ovchinnikov V V 2002 *Dokl. Phys.* **47** 302
[24] Gubernatorov V V, Sycheva T S, Dragoshanskii Yu N, Ovchinnikov V V and Ivchenko V A 2006 *Dokl. Phys.* **51** 493
[25] Bedin S A, Makhin'ko F F, Ovchinnikov V V, Gerasimenko N N and Zagorskiy D L 2017 *IOP Conf. Ser.: Mat. Sci. and Eng.* **168** 012096
[26] Didenko A N, Sharkeev Yu P, Kozlov E V and Ryabchikov A I 2004 *Long-range effects in ion-implanted metal materials* (Tomsk: NTL)
[27] Ovchinnikov V V 2018 *Surface and Coating Technology* DOI: 10.1016/j.surfcoat.2018.03.084